


Article

Susceptibility of *Staphylococcus epidermidis* to Argon Cold Plasma Jet by Oxygen Admixture

Abdel-Aleam H. Mohamed ^{1,2} , Abdulrahman H. Basher ^{1,3} , Jamal Q. M. Almarashi ¹ and Salama A. Ouf ^{4,*} 

¹ Physics Department, Faculty of Science, Taibah University, Madinah 42353, Saudi Arabia; abdelaleamm@yahoo.com (A.-A.H.M.); a.h.basher@ppl.eng.osaka-u.ac.jp (A.H.B.); almarashi@hotmail.com (J.Q.M.A.)

² Physics Department, Faculty of Science, Beni-Suef University, Beni-Suef 52511, Egypt

³ Center for Atomic and Molecular Technologies, Osaka University, Osaka 565-0871, Japan

⁴ Botany and Microbiology, Faculty of Science, Cairo University, Giza 12613, Egypt

* Correspondence: salama@sci.cu.edu.eg

Abstract: Cold atmospheric pressure sterilization is one of the nominated and efficient techniques to prevent the spread of diseases. Reactive species such as O and OH and other radicals play a major role in the mechanism of plasma sterilization. Therefore, in this work, oxygen was mixed with different parentage from (0.2 to 1.2%) to argon to enhance the generation of the reactive species and increase the argon atmospheric pressure plasma sterilization efficacy. The emission spectra from the jet increase the radicle line intensities by increasing the percentage admixture of O₂ with the argon gas to reach a maximum power at 0.8; then, it gradually decreases with a higher O₂ percentage. The OH band intensity decreases with increasing the admixture of O₂. The jet with different O₂ percentages was tested against Gram-positive *S. epidermidis*, which is the causal agent of nosocomial infections. The maximum reduction in colony-forming units (CFU) was observed at 0.2% O₂. No bacterial growth was observed at the later concentration applied for 8 min and the same case was detected at 0.4% O₂ applied to 16 min.

Keywords: cold plasma; argon; *Staphylococcus epidermidis*; bacterial susceptibility



Citation: Mohamed, A.-A.H.; Basher, A.H.; Almarashi, J.Q.M.; Ouf, S.A.

Susceptibility of *Staphylococcus epidermidis* to Argon Cold Plasma Jet by Oxygen Admixture. *Appl. Sci.* **2021**, *11*, 3455. <https://doi.org/10.3390/app11083455>

Academic Editor: Patrizia Messi

Received: 4 March 2021

Accepted: 7 April 2021

Published: 12 April 2021

Publisher's Note: MDPI stays neutral with regard to jurisdictional claims in published maps and institutional affiliations.



Copyright: © 2021 by the authors. Licensee MDPI, Basel, Switzerland. This article is an open access article distributed under the terms and conditions of the Creative Commons Attribution (CC BY) license (<https://creativecommons.org/licenses/by/4.0/>).

1. Introduction

S. epidermidis ranks first among the causative agents of nosocomial infections. Staphylococci are common bacterial colonizers of the skin and mucous membranes of humans and other mammals. *S. epidermidis* represents the most common source of infections on medical devices [1]. Therefore, prevention and considering sterilization techniques become urgent requirements to avoid the spread of the diseases. One of the efficient sterilization techniques is cold atmospheric pressure plasma sterilization [2,3].

Several techniques have been used to overcome the restrictions to generate non-thermal plasma at atmospheric pressure such as using Dielectric-barrier discharges (DBD) [4], pulsed power source [5], segmented cathode [6], and the micro-hollow cathode system [7]. Moreover, some investigators used gliding arc discharge and some others use several types of plasma jets [8]. The method by which the non-thermal atmospheric pressure plasma (APP) is generated will depend on the plasma properties required such as volume of the generated plasma, gas temperature, electron density and temperature, and homogeneity of the plasma. It is believed that a combination of the different techniques can be used to fulfill the requirement for generating non-thermal plasma with a high rate of reactive species generation and large-scale plasma.

The generation of cold atmospheric pressure plasma opened many applications in several fields including sterilization [9], medical treatment [10], and other biomedical applications [11].

Cold plasma is a new safe non-thermal sterilization technology that uses energetic, reactive gases to inactivate microbes. Atmospheric pressure plasma jets (APPJs) have been generated using low-frequency (LF) power sources in the range of kHz. Since it has a long jet, the APPJs are employed for sterilization for asymmetrical surfaces. Helium (He) plasma jet is the most stable and easiest APPJ to be generated due to its lowest breakdown voltage and lower gas temperature [4]. From the economic point of view, the use of helium is expensive; therefore, an intensive investigation has been done to find other cheaper gases such as air, nitrogen, and argon. Since air and nitrogen have a higher breakdown voltage compared to argon APPJ, argon was selected to be used instead of helium particularly for many industrial and medical purposes. Remarkably, using argon increases generated plasma gas temperature and the possibility for the glow to arc transition. Moreover, the rate of power consumption is relatively low, with high disinfection efficiency and low-cost efficacy [12].

APPJ is a kind of plasma generated at atmospheric pressure, and the plasma is formed as a phenomenon going through a jet. This type of plasma can be generated by alternating current (AC), pulsed, radio frequency (RF) as well as microwave power supplies. Currently, the characteristic properties of APPJ including its usage as a sterilization method have attracted many investigators [13–15]. Firstly, APPJ is an accessible plasma that does not need any vacuum equipment or any complex materials to be generated. Secondly, it is a flexible system that comes in a shape similar to a pin connected to the power supply and a gas cylinder. This shape gives users the possibility to bring the system into the target. Thirdly, it can be used with heat-sensitive materials including biological samples as they can not tolerate high temperature [16]. Fourthly, it is a low-cost system that just needs a very simple means to operate [17]. Finally, different operating conditions are flexible and can be changed, such as operating gases and their flow rate, the current, applied voltage, and frequency that affect the plasma characteristics and give a wide range of applications [18,19].

Non-thermal atmospheric pressure plasma jet (APPJ) can be grouped depending on the operating gas into three categories of APPJ: the noble gas plasma jet, the N₂ plasma jet, and the air plasma jet. The noble gas plasma jet is relatively the easiest kind to generate, as its breakdown voltage is less than the air and N₂, but they are not as reactive as air plasma jets. Therefore, some researchers mix the noble gases with a small percentage of reactive gases. In this case, the noble gas is used to serve as the carrier gas to generate the plasma. O₂ or H₂O₂ is often added for biomedical applications, while O₂ or CF₄ can be frequently used for applications of etching. In addition, researchers, who work on N₂ plasma jets, faced the constringent of reactive radicals too [20].

Since *S. epidermidis* infects the skin and soft tissue causing pain, swelling, warmth, and redness in the infected area [21], therefore, this work aimed to study the effect of O₂ admixture to argon non-thermal APPJ to obtain the desired reactive oxygen species (ROS) inducing maximum antibacterial activity. This treatment will allow the possibility of treatment of *S. epidermidis* infected skin. Several trials were established with different settings for the argon non-thermal APPJ to study the optimum processing conditions that accomplish the maximum bacterial inactivation.

2. Materials and Experimental Setup

2.1. Non-Thermal APPJ System

The non-thermal APPJ system consisted of an alumina ceramic (Al₂O₃) insulator tube with 150 mm length and having a 3 and 4.8 mm inner and outer diameter, respectively (Figure 1). The alumina tube has a purity of 99.7%. The tube was surrounded by two identical copper rings with a 6 mm width and 0.48 mm thickness. The two rings were separated by 10.2 mm. The lower ring was far from the tube nozzle by 5 mm and connected to the ground. A sinusoidal AC high-voltage signal was applied to the upper copper ring, which was acting as the high-voltage electrode. Argon and oxygen gases with purity 99.999% were blown through the alumina tube to form a plasma jet when the AC high

voltage was applied between its electrodes. The gas flow was controlled and measured using mass flow meters (AlicatScientific MC-5 SLPM (standard liter per minute)-D and MC-20 SLPM-D).

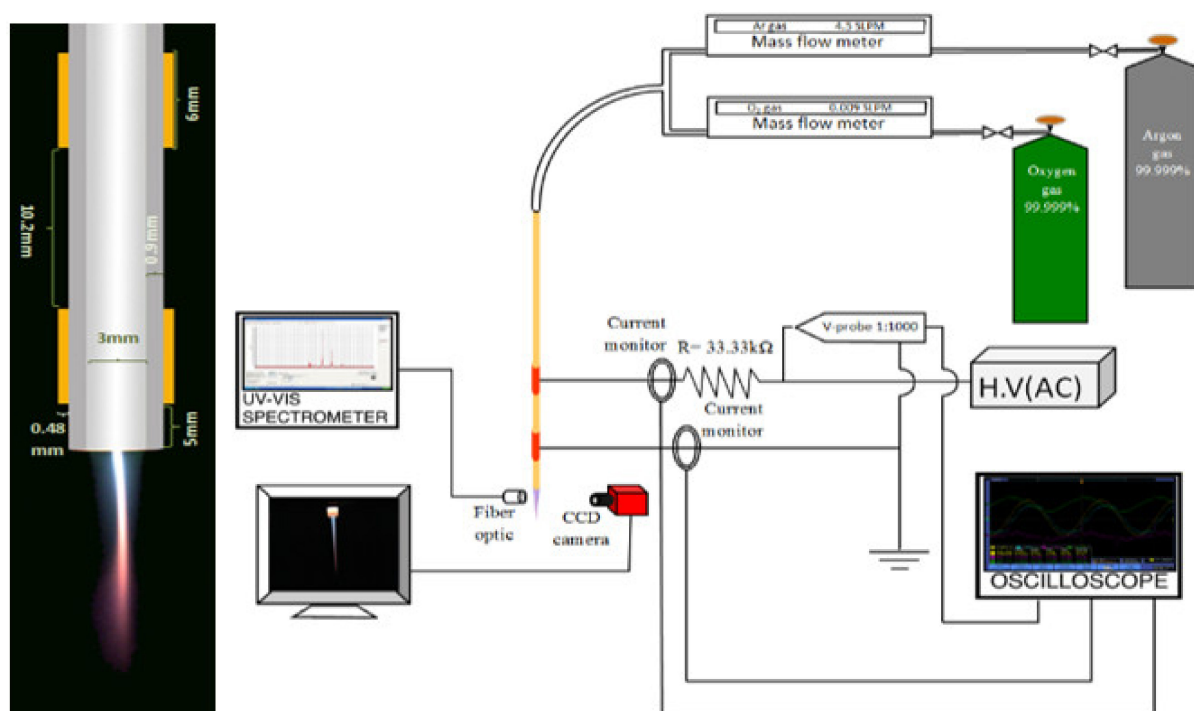


Figure 1. Experimental setup of the non-thermal APPJ with a demonstration picture to the jet at the left.

The emission spectra of non-thermal atmospheric pressure plasma jets (APPJ) in the air were characterized by optical emission spectroscopy using an Acton SP-2356 imaging spectrograph with a single-leg-fiber optic bundle (LG-455-020-3). It is a triple grating 500 mm focal length spectrograph. Two gratings were used throughout this work. The first grating has 3600 gr/mm, which is blazed at 253.65 nm and sensitive in the range 200–450 nm, the second grating has 1800 gr/mm, which is blazed at 500 nm, and its sensitivity range is 450–850 nm. The third grating—which was not used—has 150 gr/mm and is blazed at 1000 nm with a sensitive range of 615–1800 nm. The spectrograph was equipped with a built-in high sensitive photomultiplier detector with a sensitivity range from 190 to 900 nm (model ARC-P2, Princeton instrument).

The gas temperature of the non-thermal APPJ was measured by evaluating the rotational (0,0) band of the second positive N_2 system. The recorded spectrum was observed side-on, from the nitrogen second positive system N_2 ($C^3\Pi_u-B^3\Pi_g$), and compared to a simulated spectrum. Then, the temperature was attained by matching the two spectra. Moreover, the vibrational temperature (T_{vib}) was measured by comparing the experimental emission spectra of the argon non-thermal APPJ with the simulated one.

2.2. Biological Measurements Set-Up

2.2.1. Test Organism

S. epidermidis was used as a test organism. The bacterium was kindly provided from the reference laboratory in Almadinah Almunawwarah, Saudi Arabia. The bacterial species were cultured on Petri dishes with basic medium (BM: 1% peptone, 0.5% yeast extract, 0.1% glucose, 0.5% NaCl, 0.1% K_2HPO_4).

2.2.2. Treatments and Bacterial Count

The bacterial suspension was prepared from *S. epidermidis* culture previously grown on the basic medium for 48 h. The concentration of bacteria was adjusted at 78×10^6 colony-

forming units (CFU)/ml. Preliminary trials were made to adjust the concentration using spectrophotometric and dilution plate methods. Then, the bacterial suspension was distributed into sterile Eppendorf tubes of 2 mL capacity. Then, the tubes were exposed to pure argon plasma and argon plasma mixed with 0.2, 0.4, 0.6, 0.8, 1.0, and 1.2% oxygen. The plasma-emitting jet outlet was located 0.5 cm outside the tubes containing the bacterial suspension in a sealed atmosphere. The exposure times for each concentration ranged from 1 to 16 min. By the end of exposure time, 0.5 mL portions of the treated bacterial suspension were transferred and spread onto Petri plates containing the basic agar medium. Four replicates were used for each treatment. The plates were incubated at 25 °C for 48 h. Then, the grown CFUs were counted using a bacterial colony counter with the help of a transmission light array and magnifier hand counter.

3. Results and Discussion

3.1. The Effect of Oxygen Gas Mixing on ACPPJ

The generated reactive species (OH, NO, O) from the non-thermal APPJ can be enhanced by mixing the input gas with other gases. Therefore, oxygen gas is added with different ratios to reach optimum O-radical production [20]. The occurrence of oxygen causes all plasma processes rather complex, even in a simple binary gas mixture [22]. The effect of adding oxygen gas electrically and optically is presented in this section.

Mixing oxygen gas with argon to generate non-thermal APPJ may seem quite obvious, as shown in Figure 2, which presents the current–voltage waveforms with pure argon in (a) and 0.4 % oxygen (0.018/4.5 slpm) mixed in (b) at fixed ≈ 14 kV and 29 kHz. Through this work, argon gas was mixed with oxygen at 4.5 argon flow rate. The current values presented in this work are the current peak values. Adding oxygen gas increases the total current from ≈ 11.3 to ≈ 18 mA while the ground current increased from ≈ 8.3 to ≈ 22.9 mA, which is slightly higher than the total current for the positive half cycle. For the negative half cycle, the total current rises from ≈ 11.6 to ≈ 17.2 mA and from ≈ 8.1 to ≈ 16.6 mA for the ground one. Moreover, the number of currents peaks for each half cycle normally increases with applied voltage [23]. However, the current–voltage waveform in case of mixing oxygen is presenting the same effect of increasing the current peaks per each half cycle, and this effect could be due to the increase in the residual charge carriers from the privies pulse owing to oxygen electron affinity [20].

The imaging of the non-thermal APPJ declared that adding oxygen to the plasma accelerates the mode transition from filamentary to diffused mode at lower flow rate values compared to the case of pure argon as illustrated in Figure 3. Normally, the filament is generated inside the diffused plasma at the operation condition 4.5 slpm, 14 kV, and 29 kHz [24]. However, the filament is disappearing by adding oxygen gas. Moreover, increasing the mixing of oxygen gas to the argon non-thermal APPJ causes the shrink of the plasma plume length.

Figure 4 shows the generated non-thermal APPJ emission spectra in the ranges from 200 to 450 nm (Figure 4a) and from 450 to 850 nm (Figure 4b) at different O₂ mixture percentages from 0.2% to 1.2%. The emission spectra for pure argon flow show the domination of the nitrogen second positive system in the range from 300 to 450 nm, while Ar lines were the highest intensity in the range from 600 to 850 nm. As the oxygen percentage increases, the plasma plume intensity decreases, and that takes place on the emission spectra. The band and line intensities decrease by increasing the percentage of oxygen into the argon gas, as shown in Figure 4. Moreover, adding oxygen gas lets the three lines of oxygen spectrum be emitted clearly at 777.35, 777.6, and 777.7 nm as well as the fourth one at 844.80 nm, as shown in Figure 5. The measurements of the gas temperature and vibrational temperature result in an estimated 320 K gas temperature (rotational temperature) and 1200 K vibrational temperature. The estimated temperature results from the comparison between the measured and the simulated spectra for pure Ar and Ar + 0.2% O₂ at 14 kV peak-to-peak voltage and 29 kHz. These measurements prove that the generated plasma is non-thermal equilibrium plasma.

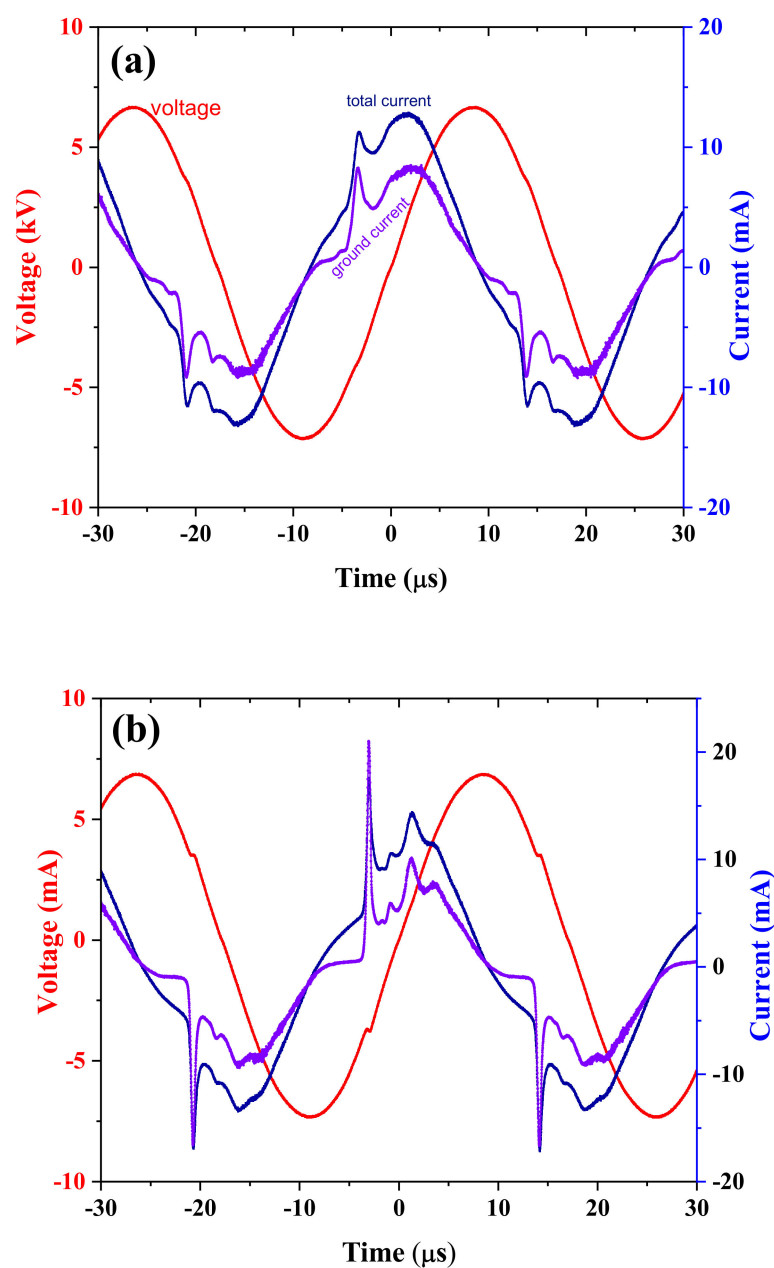


Figure 2. Current-voltage waveforms with (a) pure argon and (b) mixed with 0.018 slpm (0.4%) oxygen to 4.5 slpm argon flow rate, ≈ 14 kV and 29 kHz.

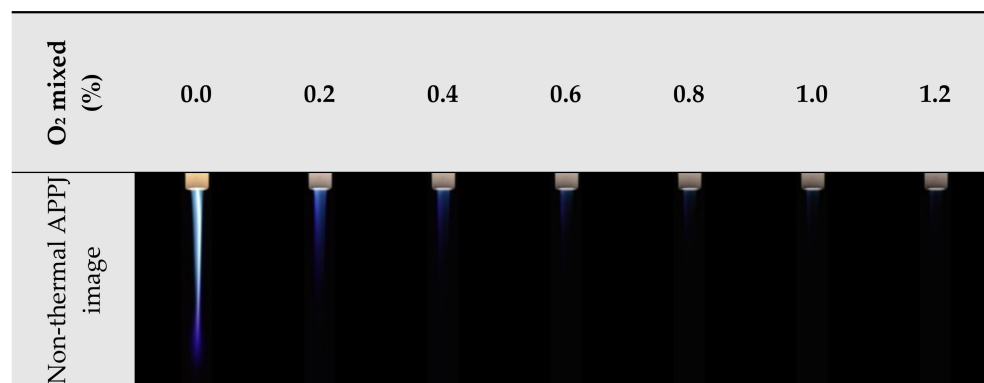


Figure 3. Non-thermal APPJ images show its development as a fraction of increasing the oxygen percentages, operating at fixed 14 kV and 29 kHz, and 4.5 slpm argon flow.

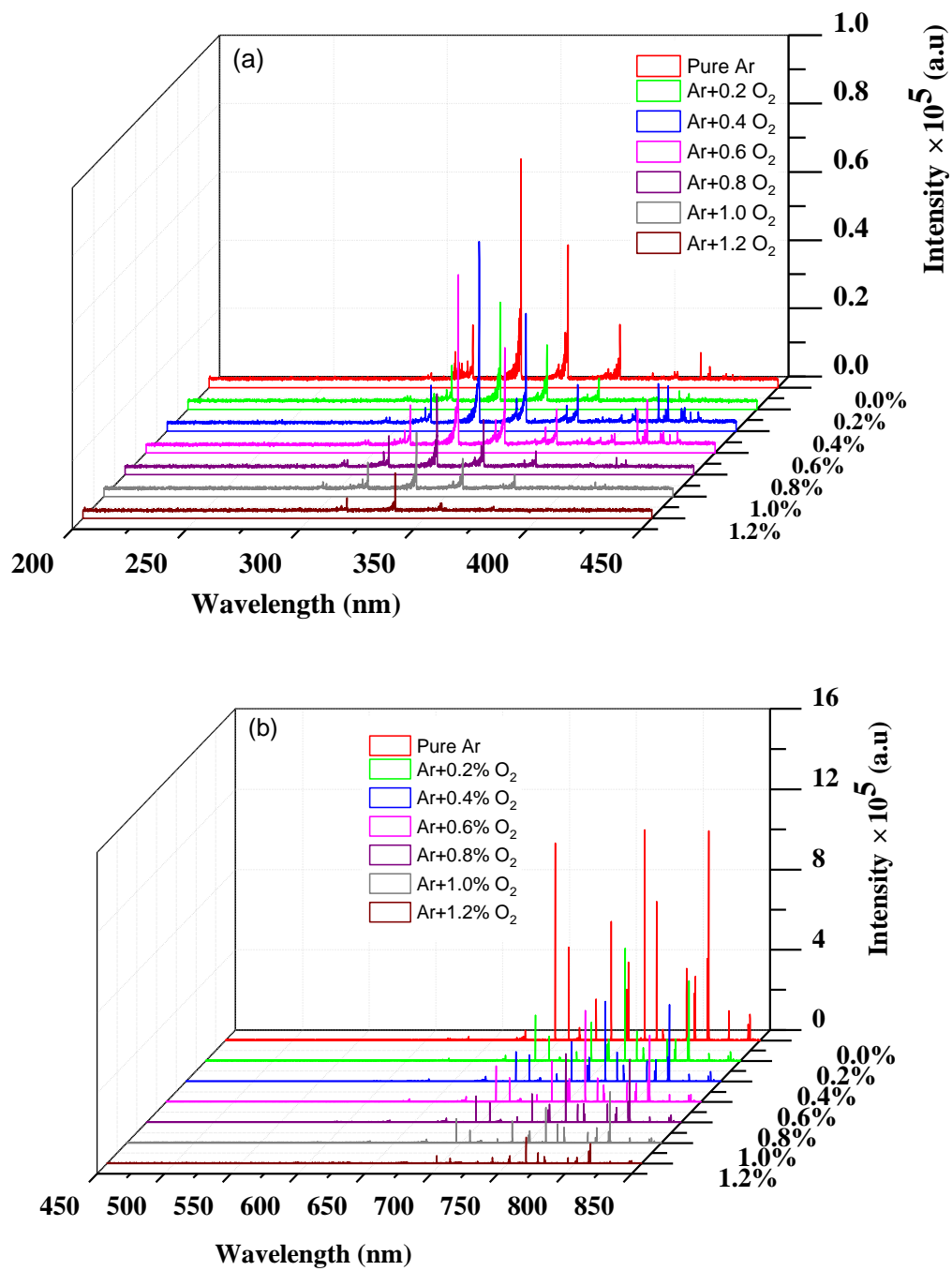


Figure 4. Emission spectra of the argon non-thermal APPJ in the range 200–850 nm at 14 kV, 29 kHz, and 4.5 slpm with different oxygen concentrations (a) and (b).

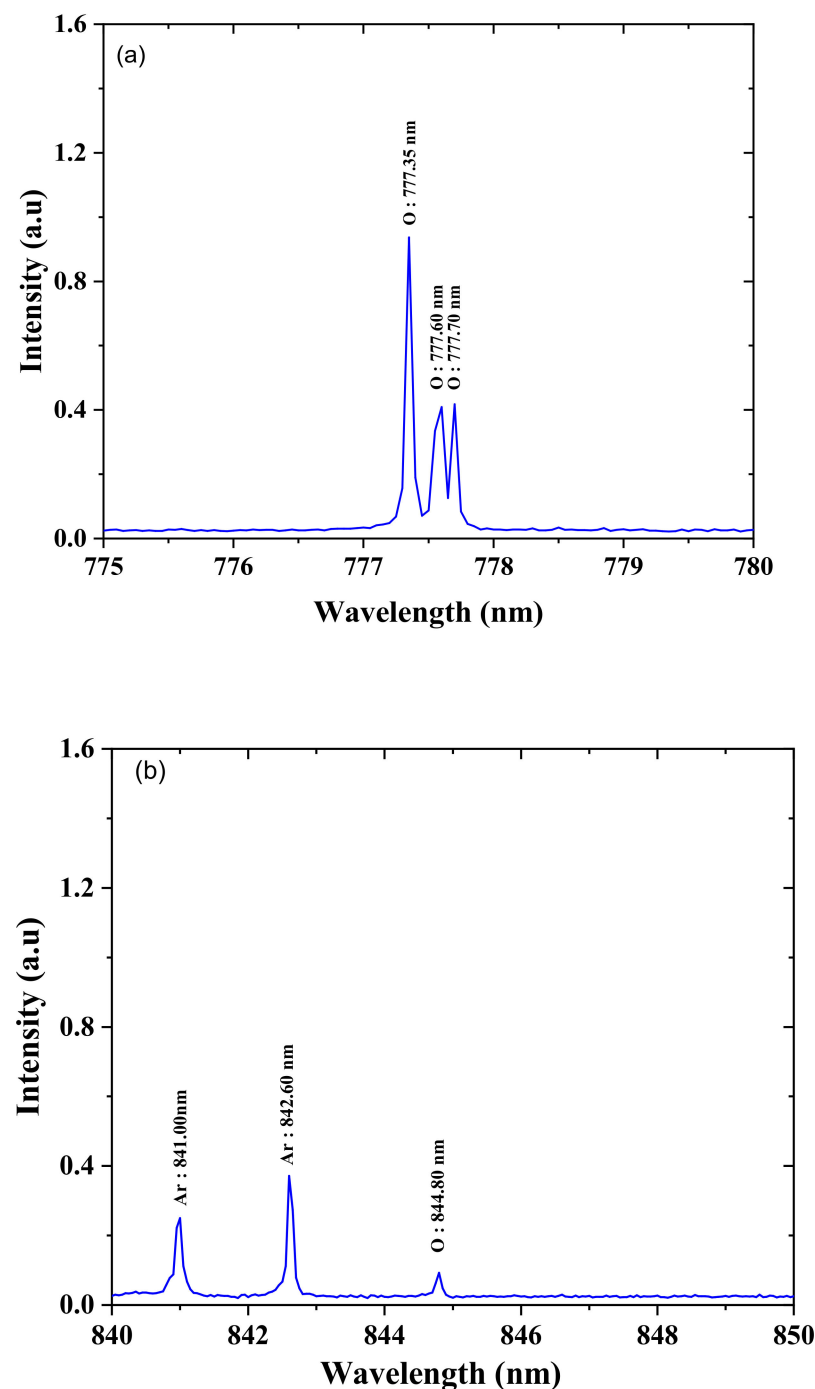


Figure 5. The emission spectrum of the oxygen lines at 14 kV, 29 kHz, and 4.5 slpm argon mixed with 0.036 slpm (0.8%) oxygen (a) and (b).

The oxygen radical line intensities increase by increasing the addition of O_2 to reach the maximum at 0.8%. Then, it decreases with increasing O_2 percentage. A similar trend was reported for RF helium discharge with maximum consideration of radical at 0.5% of O_2 admixture [25]. The OH-radical band intensity was measured by the summation of the intensity of the OH band from 305 to 315 nm. The obtained OH intensity measurements show an almost linear decrease with increasing the O_2 mixture, as shown in Figure 6. This decrease in OH intensity is due to the loss of electrons in the discharge zone, with higher oxygen percentage due to the attachment of electrons with oxygen. Previous studies show that OH was quenched by O through the reaction ($OH + O \rightarrow O_2 + H$) [26].

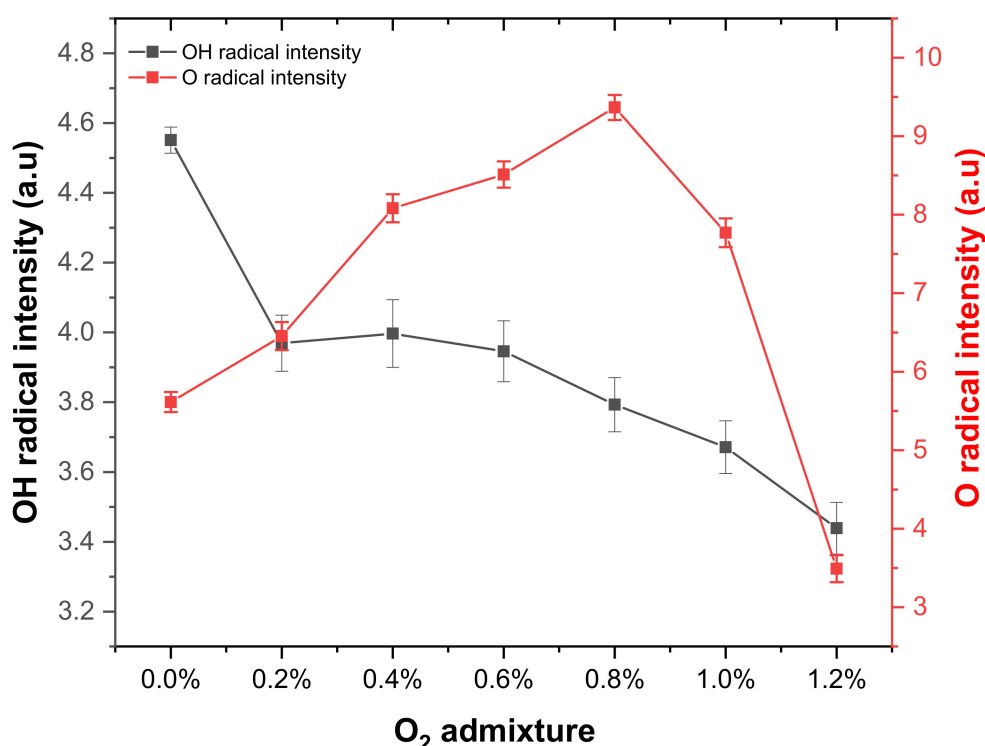


Figure 6. Effect of O₂ admixture variation on atomic O and OH radical intensities at 2 mm below the jet nozzle at fixed 14 kV and 29 kHz.

Oxygen is electronegative gas, and its mixing with the operating argon gas increases electron losses due to attachment. Oxygen mixture contributes to energy losses for electrons, the number of excitations, ionization, and dissociation processes [20]. These all contribute to lowering the electron temperature with just a little oxygen introduced [22]. Nevertheless, electron collisions with oxygen efficiently promote a variety of positive and negative ions (O⁺, O₂⁺, O₄⁺, O₃[−], O₂[−], O[−]) [22]. These oxygen-related ions can all effectively contribute to increasing the gas temperature. In particular, dissociative electron attachment leading to O[−] + O is very effective and is activated at energy as low as 5 eV [23]. This dissociative process can reduce electron energy, decrease electron density, and contribute to channel energy into heating the gas at the same time [22]. The characteristic properties of oxygen and its electronegativity seem to be responsible for transferring energy from electrons to an overall increased gas temperature [22].

There is no significant change in the electron energy distribution function (EEDF) with a small O₂ admixture. Therefore, with increasing the O₂, the dissociation increases until the rotational and vibrational molecular excitations and the electron attachment cause a significant energy loss. This loss causes a change and decreases the dissociation rate, leading to a decrease in the O concentration, which is started at 0.8% of O₂ admixture [26].

3.2. Anti-Bacterial Activity of Non-Thermal APPJ

The application of a cold plasma device as an antibacterial and safety agent for the stimulation of wound healing was recently tested by Boekema et al. [27] using human dermal samples. Their study demonstrated the in vitro and in vivo safety and efficacy in *Staphylococcus aureus* reduction by using a flexible dielectric barrier discharge plasma device.

The effect of non-thermal APPJ using pure argon and argon mixed with oxygen molecules on the reduction of colony-forming units (CFUs) of *S. epidermidis* count is shown in Figure 7. There is a steady decrease in the count of *S. epidermidis* under all treatments with the maximum reduction achieved for the non-thermal APPJ when argon is mixed with 0.2% oxygen. The reduction for later cases was dropped from 78×10^6 CFU/mL (initial count) to 1.2×10^6 CFU/mL as compared to 2.9×10^6 for pure argon plasma delivered for

one minute. Increasing the addition of oxygen to the argon lowered the toxicity of the pure argon plasma where the CFUs of *S. epidermidis* recorded $3.3, 3.5, 3.9$, and 4.3×10^6 CFU/mL after one minute for the plasma-derived from argon mixed with 0.6%, 0.8%, 1.0%, and 1.2% oxygen, respectively. Generally, the extension of exposure time, under different treatments, from 1 up to 16 min leads to a gradual increase in the reduction of CFU of *S. epidermidis* reaching 0.9×10^6 CFU/mL for pure argon plasma after 16 min. However, there is a steady decrease in the count of *S. epidermidis* from 78×10^6 to 3.5×10^6 CFU/mL on exposure to plasma for 1 min using pure argon as operating gas. The maximum reduction in CFU was observed at 0.2% O₂. No bacterial growth was observed at the later concentration applied for 8 min and the same case was detected at 0.4% O₂ applied to 16 min.

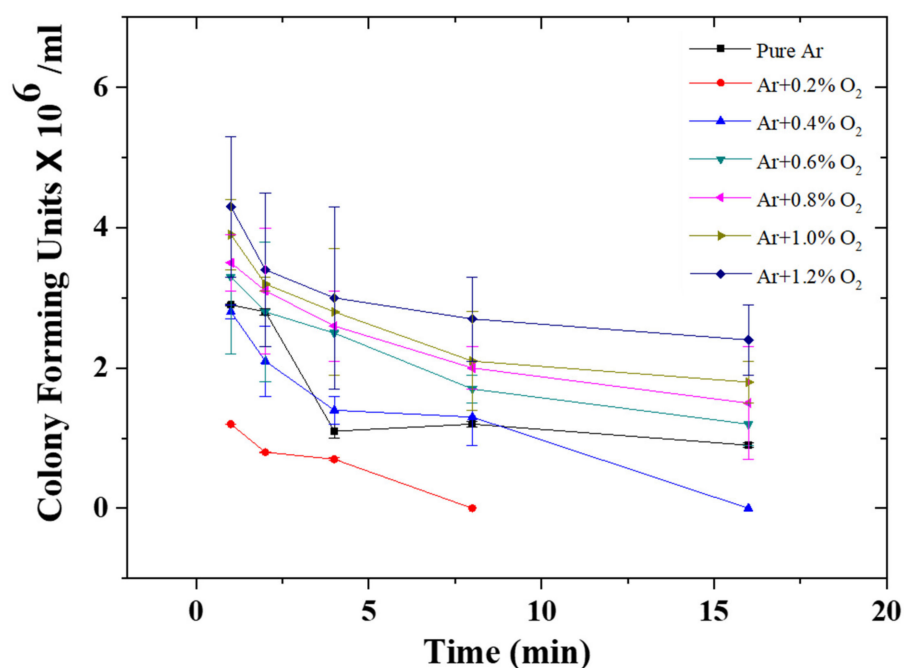


Figure 7. Effect of argon non-thermal APPJ generated at different oxygen admixtures (0.2 to 1.2%) on the colony-forming unit (CFU) $\times 10^6$ /mL of *S. epidermidis* at different exposure times.

Matthes et al. [28] tried cold atmospheric pressure argon plasma against 78 genetically different *S. aureus* strains for clinical and epidemiological implications. Their study established the high complexity of microbial defense against antimicrobial treatment and strain-dependent susceptibility of *S. aureus* to plasma treatment.

Several authors indicated that the degree of microbial inactivation probably depends on the type of micro-organisms, the inactivation medium, number of cells, operating gas mixture, gas flow, and physiological state of cells [29,30]. The difference in the effectiveness of each treatment or operating gas mixture is probably related to the emitted reactive species produced by the atmospheric plasma. The anti-bacterial activity of the cold plasma is probably due to the generation of oxygen and OH-radicals, which are almost produced in an equal amount at argon mixed with 0.2% oxygen, as shown in the spectroscopic measurements.

The intense bombardment of the generated radicals with the bacterial cell walls induces severe irreversible cell wall damage, leading to its destruction [31]. In previous works [32–35], the antimicrobial effectiveness of charged particles, free radicals, and UV-emitting species was described. Moreover, the cold atmospheric plasma may induce destruction in cellular constructions and cell permeation [36] as well as destruction and cracking of the cell walls or cell membrane of micro-organisms [37]. In addition, Takeda et al. [38] showed that the energized electrons and ions could collide with organic molecules on the cell and disrupt the chemical bonds and induce perforations to the cell membrane. Moreover, the reactive oxidizing agents and reactive nitrogen species (e.g., ROS and RNS) produced in APPJ could react with and damage the cell or the contents. In an in vitro

test [39], the researchers showed that cold atmospheric argon plasma applied for 25 min at the 40 W was lethal for the growth of *Aspergillus flavus* on the medium, while the application of plasma for 20 min at the same voltage was important in the protection of brown rice cereal bars from the contamination of *A. flavus* up to 20 days under storage conditions of 25 °C and 100% relative humidity. The longer treatment time, as compared with our data (16 min), is probably due to the high voltage they employed.

Critzer et al. [40] have reported the ability of atmospheric plasma for the decrease of microbial populations on surfaces of fresh produce. Fernandez et al. [41] stated that cold atmospheric gas plasma applied for 15 min accomplished 2.72, 1.76, and 0.94 log-reductions of *Salmonella typhimurium* on lettuce, strawberry, and potato, respectively. It is suggested that the electrostatic force caused by charge accumulation on the outer surface of the cell membrane weakens the tensile strength of the membrane, thus initiating its rupture [34,42].

In a related study, Nicol et al. [43] investigated the efficacy of low-temperature plasma treatments against bacteria using an atmospheric-pressure plasma jet and show that plasma treatments can inhibit both Gram-positive (*S. aureus*) and Gram-negative (*E. coli*) bacteria on solid and porous surfaces. Moreover, both direct plasma treatment and plasma-activated media were effective against the bacteria suspended in liquid culture. They also indicated that reactive oxygen species are the key mediators of the bactericidal effects of cold plasma, and the presence of hydrogen peroxide is necessary but not sufficient for antibacterial effects. In addition, they suggest that bacteria exposed to plasma do not develop resistance to further treatment.

4. Summary

As a new tool of disinfection technology, a non-thermal APP system was investigated as an effective technique by mixing O₂ to the operating argon gas. The effects of O₂ admixture from 0.2% to 1.2% were investigated on the plasma formation, current–voltage waveforms, and emission spectra. The ground and total current peaks for positive and negative half cycle were increased considerably by increasing the addition of the O₂. The plasma plume intensity and emission spectra intensity decrease with increasing the O₂ admixture. The emission spectra intensity of O-radicle increases with increasing O₂ to reach a maximum of 0.8%; then, it decreases with a higher percentage of O₂. However, the emission spectrum from the OH band decreases with increasing the addition of O₂. The non-thermal APPJ different O₂ admixture was used to successfully disinfect *S. epidermidis*. There was a steady decrease CFU of *S. epidermidis* under all treatments with maximum reduction at 0.2% oxygen. This reduction was from 78×10^6 CFU/mL (initial count) to 1.2×10^6 CFU/mL, as compared to 2.9×10^6 CFU/mL for pure argon non-thermal APPJ delivered for one-minute exposure. A multi-jet system was demonstrated as an example for the lateral expansion of a single jet.

Author Contributions: Conceptualization, A.-A.H.M., J.Q.M.A., and S.A.O.; methodology, A.-A.H.M., A.H.B. and S.A.O.; writing—original draft preparation, A.-A.H.M., A.H.B. and S.A.O.; writing—review and editing, A.-A.H.M. and S.A.O.; All authors have read and agreed to the published version of the manuscript.

Funding: This work was partially supported by the Japan Society for the Promotion of Science (JSPS) Research Fellowship for Young Scientist Program (No. 20J10393).

Institutional Review Board Statement: Not applicable.

Informed Consent Statement: Not applicable.

Data Availability Statement: Not applicable.

Acknowledgments: The authors appreciate the support from the Unit of Science and Technology, Taibah University, Saudi Arabia.

Conflicts of Interest: The authors declare no conflict of interest.

References

- Brown, M.M.; Horswill, A.R. Staphylococcus epidermidis—Skin friend or foe? *PLoS Pathog.* **2020**, *16*, e1009026. [\[CrossRef\]](#)
- Guo, L.; Xu, R.; Gou, L.; Liu, Z.; Zhao, Y.; Liu, D.; Zhang, L.; Chen, H.; Kong, M.G. Mechanism of Virus Inactivation by cold atmospheric-pressure plasma and plasma-activated water. *Appl. Environ. Microbiol.* **2018**, *84*. [\[CrossRef\]](#) [\[PubMed\]](#)
- Xia, T.; Kleinheksel, A.; Lee, E.M.; Qiao, Z.; Wigginton, K.R.; Clack, H.L. Inactivation of airborne viruses using a packed bed non-thermal plasma reactor. *J. Phys. D Appl. Phys.* **2019**, *52*, 255201. [\[CrossRef\]](#) [\[PubMed\]](#)
- Kogelschatz, U. Dielectric-barrier discharges: Their history, discharge physics, and industrial applications. *Plasma Chem. Plasma Process.* **2003**, *23*, 1–46. [\[CrossRef\]](#)
- Tsigutkin, K.; Kroupp, E.; Stambulchik, E.; Osin, D.; Doron, R.; Arad, R.; Starobinets, A.; Maron, Y.; Uschmann, I.; Förster, E.; et al. Diagnostics and investigations of the plasma and field properties in pulsed-plasma configurations. *IEEE Trans. Fundam. Mater.* **2004**, *124*, 501–508. [\[CrossRef\]](#)
- Donko, Z.; Apai, P.; Szalai, L.; Rozsa, K.; Tobin, R. The segmented hollow cathode discharge: A pumping source for UV metal ion lasers. *IEEE Trans. Plasma Sci.* **1996**, *24*, 33–34. [\[CrossRef\]](#)
- Mahony, C.M.O.; Gans, T.; Graham, W.G.; Maguire, P.D.; Petrović, Z.L. Ultrasmall radio frequency driven microhollow cathode discharge. *Appl. Phys. Lett.* **2008**, *93*, 11501. [\[CrossRef\]](#)
- Rauscher, H.; Perucca, M.; Buyle, G. *Plasma Technology for Hyperfunctional Surfaces: Food, Biomedical and Textile Applications*; Wiley: New York, NY, USA, 2010.
- Moisan, M.; Barbeau, J.; Crevier, M.-C.; Pelletier, J.; Philip, N.; Saoudi, B. Plasma sterilization. Methods and mechanisms. *Pure Appl. Chem.* **2002**, *74*, 349–358. [\[CrossRef\]](#)
- Lu, X.; Jiang, Z.; Xiong, Q.; Tang, Z.; Pan, Y. A single electrode room-temperature plasma jet device for biomedical applications. *Appl. Phys. Lett.* **2008**, *92*, 151504. [\[CrossRef\]](#)
- Laroussi, M.; Hynes, W.; Akan, T.; Lu, X.; Tendero, C. The plasma pencil: A source of hypersonic cold plasma bullets for biomedical applications. *IEEE Trans. Plasma Sci.* **2008**, *36*, 1298–1299. [\[CrossRef\]](#)
- Korolev, Y.D.; Mesyats, G.A. *Physics of Pulsed Breakdown in Gases*; Ural Division of the Russian Academy of Science: Ekaterinburg, Russia, 1998.
- Nan, J.; Ji, A.; Cao, Z. Atmospheric pressure plasma jet: Effect of electrode configuration, discharge behavior, and its formation mechanism. *J. Appl. Phys.* **2009**, *106*, 013308.
- Puač, N.; Maletić, D.; Lazović, S.; Malović, G.; Đorđević, A.; Petrović, Z. Current–voltage characteristics of atmospheric pressure plasma jet. *Publ. Astron. Obs. Belgrade* **2010**, *89*, 307–310.
- Xian, Y.; Wu, S.; Wang, Z.; Huang, Q.; Lu, X.; Kolb, J.F. Discharge dynamics and modes of an atmospheric pressure non-equilibrium air plasma jet. *Plasma Process. Polym.* **2013**, *10*, 372–378. [\[CrossRef\]](#)
- Wu, S.; Xu, H.; Lu, X.; Pan, Y. Effect of pulse rising time of pulse dc voltage on atmospheric pressure non-equilibrium plasma. *Plasma Process. Polym.* **2013**, *10*, 136–140. [\[CrossRef\]](#)
- Xian, Y.; Lu, X.; Tang, Z.; Xiong, Q.; Gong, W.; Liu, D.; Jiang, Z.; Pan, Y. Optical and electrical diagnostics of an atmospheric pressure room-temperature plasma plume. *J. Appl. Phys.* **2010**, *107*, 063308. [\[CrossRef\]](#)
- Feng, H.; Sun, P.; Chai, Y.; Tong, G.; Zhang, J.; Zhu, W.; Fang, J. The interaction of a direct-current cold atmospheric-pressure air plasma with bacteria. *IEEE Trans. Plasma Sci.* **2008**, *37*, 121–127. [\[CrossRef\]](#)
- Machala, Z.; Hensel, K.; Akishev, Y. *Plasma for Bio-Decontamination, Medicine and Food Security*; Springer: Berlin/Heidelberg, Germany, 2012.
- Lu, X.; Laroussi, M.; Puech, V. On atmospheric-pressure non-equilibrium plasma jets and plasma bullets. *Plasma Sources Sci. Technol.* **2012**, *21*, 034005. [\[CrossRef\]](#)
- Byrd, A.L.; Belkaid, Y.; Segre, J.A. The human skin microbiome. *Nat. Rev. Microbiol.* **2018**, *16*, 143–155. [\[CrossRef\]](#) [\[PubMed\]](#)
- Mariotti, D.; Shimizu, Y.; Sasaki, T.; Koshizaki, N. Gas temperature and electron temperature measurements by emission spectroscopy for an atmospheric microplasma. *J. Appl. Phys.* **2007**, *101*, 013307. [\[CrossRef\]](#)
- Becker, K.; Kogelschatz, U.; Schoenbach, K.; Barker, R. *Non-Equilibrium Air Plasmas at Atmospheric Pressure*; IOP: Bristol, UK, 2005.
- Basher, A.H.; Mohamed, A.-H. Laminar and turbulent flow modes of cold atmospheric pressure argon plasma jet. *Polymers* **2018**, *9*, 630. [\[CrossRef\]](#)
- Knake, N.; Reuter, S.; Niemi, K.; Der Gathen, V.S.-V.; Winter, J. Absolute atomic oxygen density distributions in the effluent of a microscale atmospheric pressure plasma jet. *J. Phys. D Appl. Phys.* **2008**, *41*. [\[CrossRef\]](#)
- Lu, X.; Naidis, G.; Laroussi, M.; Reuter, S.; Graves, D.; Ostrikov, K. Reactive species in non-equilibrium atmospheric-pressure plasmas: Generation, transport, and biological effects. *Phys. Rep.* **2016**, *630*, 1–84. [\[CrossRef\]](#)
- Boekema, B.; Stoop, M.; Vlig, M.; van Liempt, J.; Sobota, A.; Ulrich, M.; Middelkoop, E. Antibacterial and safety tests of a flexible cold atmospheric plasma device for the stimulation of wound healing. *Appl. Microbiol. Biotechnol.* **2021**, *105*, 2057–2070. [\[CrossRef\]](#) [\[PubMed\]](#)
- Matthes, R.; Lührman, A.; Holtfreter, S.; Kolata, J.; Radke, D.; Hübner, N.-O.; Assadian, O.; Kramer, A. Antibacterial activity of cold atmospheric pressure argon plasma against 78 genetically different (mecA, luk-P, agr or capsular polysaccharide type) staphylococcus aureus strains. *Ski. Pharmacol. Physiol.* **2016**, *29*, 83–91. [\[CrossRef\]](#)

29. Song, S.H.; Park, K.U.; Lee, J.H.; Kim, E.C.; Kim, J.Q.; Song, J. Electrospray ionization-tandem mass spectrometry analysis of the mycolic acid profiles for the identification of common clinical isolates of mycobacterial species. *J. Microbiol. Methods* **2009**, *77*, 165–177. [[CrossRef](#)] [[PubMed](#)]
30. Yu, H.; Perni, S.; Shi, J.; Wang, D.; Kong, M.; Shama, G. Effects of cell surface loading and phase of growth in cold atmospheric gas plasma inactivation of *Escherichia coli* K12. *J. Appl. Microbiol.* **2006**, *101*, 1323–1330. [[CrossRef](#)]
31. Montie, T.; Kelly-Wintenberg, K.; Roth, J. An overview of research using the one atmosphere uniform glow discharge plasma (OAUGDP) for sterilization of surfaces and materials. *IEEE Trans. Plasma Sci.* **2000**, *28*, 41–50. [[CrossRef](#)]
32. Ouf, S.A.; El-Adly, A.A.; Mohamed, A.-A.H. Inhibitory effect of silver nanoparticles mediated by atmospheric pressure air cold plasma jet against dermatophyte fungi. *J. Med. Microbiol.* **2015**, *64*, 1151–1161. [[CrossRef](#)]
33. Mohamed, A.-A.H.; Al-Mashraqi, A.A.; Shariff, S.M.; Benghanem, M.; Basher, A.H.; Ouf, S.A. Generation of large volume atmospheric pressure air plasma. *IEEE Trans. Plasma Sci.* **2014**, *42*, 2488–2489. [[CrossRef](#)]
34. Laroussi, M.; Lu, X.; Malott, C.M. A non-equilibrium diffuse discharge in atmospheric pressure air. *Plasma Sources Sci. Technol.* **2003**, *12*, 53–56. [[CrossRef](#)]
35. El-Sayed, W.; Ouf, S.; Mohamed, A.H. Deterioration to extinction of wastewater bacteria by non-thermal atmospheric pressure air plasma as assessed by 16s rDNA-DGGE fingerprinting. *Front. Microbiol.* **2015**, *6*, 1098. [[CrossRef](#)]
36. Ohkawa, H.; Akitsu, T.; Tsuji, M.; Kimura, H.; Kogoma, M.; Fukushima, K. Pulse-modulated, high-frequency plasma sterilization at atmospheric-pressure. *Surf. Coat. Technol.* **2006**, *200*, 5829–5835. [[CrossRef](#)]
37. Yang, L.; Chen, J.; Gao, J. Low temperature argon plasma sterilization effect on *Pseudomonas aeruginosa* and its mechanisms. *J. Electrostat.* **2009**, *67*, 646–651. [[CrossRef](#)]
38. Takeda, K.; Yamada, H.; Ishikawa, K.; Sakakita, H.; Kim, J.; Ueda, M.; Ikeda, J.-I.; Akimoto, Y.; Kataoka, Y.; Yokoyama, N.; et al. Systematic diagnostics of the electrical, optical, and physicochemical characteristics of low-temperature atmospheric-pressure helium plasma sources. *J. Phys. D Appl. Phys.* **2019**, *52*, 165202. [[CrossRef](#)]
39. Suhem, K.; Matan, N.; Nisoa, M.; Matan, N. Inhibition of *Aspergillus flavus* on agar media and brown rice cereal bars using cold atmospheric plasma treatment. *Int. J. Food Microbiol.* **2013**, *161*, 107–111. [[CrossRef](#)] [[PubMed](#)]
40. Critzer, F.J.; Kelly-Wintenberg, K.; South, S.L.; Golden, D.A. Atmospheric plasma inactivation of foodborne pathogens on fresh produce surfaces. *J. Food Prot.* **2007**, *70*, 2290–2296. [[CrossRef](#)] [[PubMed](#)]
41. Fernández, A.; Noriega, E.; Thompson, A. Inactivation of salmonella enterica serovar typhimurium on fresh produce by cold atmospheric gas plasma technology. *Food Microbiol.* **2013**, *33*, 24–29. [[CrossRef](#)] [[PubMed](#)]
42. Mendis, D.A.; Rosenberg, M.; Azam, F. A note on the possible electrostatic disruption of bacteria. *IEEE Trans. Plasma Sci.* **2000**, *28*, 1304–1306. [[CrossRef](#)]
43. Nicol, M.J.; Brubaker, T.R.; Ii, B.J.H.; Simmons, A.N.; Kazemi, A.; Geissel, M.A.; Whalen, C.T.; Siedlecki, C.A.; Bilén, S.G.; Knecht, S.D.; et al. Antibacterial effects of low-temperature plasma generated by atmospheric-pressure plasma jet are mediated by reactive oxygen species. *Sci. Rep.* **2020**, *10*, 1–11. [[CrossRef](#)]